

Microfluidic Device

A fully automated device for ECM synthesis

Final Report

Biomedical Engineering Design 301
Department of Biomedical Engineering
University of Wisconsin
April 29, 2020

Team Members:

Jason Wang (Leader)
Nick Pauly (Communicator)
Kevin Koesser (BWIG)
Bob Meuler (BSAC)
Jiacomo Beckman (BPAG)

Client:

Dr. Paul Campagnola
Department of Biomedical Engineering

Advisor:

Assistant Professor Dr. Filiz Yesilkoy
Department of Biomedical Engineering
University of Wisconsin Madison

Abstract

Dr. Campagnola's lab has designed and constructed several microscope-based instruments for creating 3D nano/microstructure tissue engineered scaffolds. These are used for studying cell-extracellular (ECM) interactions in cancers and fibrosis as well as for general biology applications. The protein solution for the engineered scaffold varies -- either Fibronectin, Laminin 1 (alpha 1, beta 1, gamma 1) or Collagen type 1. A series of photochemistry reactions that result in the generation of a radical of a particular protein links to a second protein molecule in solution and generates a covalent bond. Using the lab's current methods, this process is repeated over 3 hours in order to generate a full ECM scaffold. The client seeks an automated system capable of introducing protein solution, filtering excess precipitate, and recovering unpolymerized protein solutions for re-use. After a series of designs, a system using a multichannel pump in conjunction with a microfluidic device that has a built in filtering system was created. The microfluidic device was planned to be tested in-field. However, due to unprecedented circumstances, theoretical analysis of the design was conducted instead to gain insight towards the validity of the device.

Table of Contents

Abstract	2
Table of Contents	3
I. Introduction	5
Problem Statement	5
II. Background	6
Client Information	6
Extracellular Matrix Imaging	6
Modulated Raster Scanning	6
Summary of Product Design Specifications	8
Summary of Previous Semester's Work	8
III. Preliminary Designs	12
Weights	12
Clamp	12
Magnets	13
IV. Preliminary Design Evaluation	13
Design Matrices Summary	13
Design Matrix	14
V. Fabrication/Development Process	15
Materials	15
Final Design	16
VI. Testing & Results	17
Testing Protein Adsorption	17
Velocity and Pressure Profile Inside Tubing	18
Simulation of Pressure in Microfluidic Device	19
VII. Discussion	20
Protein Adsorption Test	20
Future Work	20
VIII. Conclusion	21
IX. References	22
X. Appendices	23
Appendix A: Product Design Specification (PDS)	23

Appendix B: Expenses and Purchases	27
Appendix C: Mathematical Derivation	29
Appendix D: EPU-40 vs SIL-30 Report for Midwest Prototype	30

I. Introduction

Dr. Paul Campagnola and his lab focuses on studying the alterations of extracellular matrix (ECM) in epithelial cancers as well as in connective tissue disorders. His lab aims to better understand the “structural organization and cell-matrix interactions (that) could lead to the development of more efficacious treatments [1].” To study these processes, Dr. Campagnola’s lab uses Second Harmonic Generation imaging microscopy to image structural aspects of the ECM. Consequently, they are able to utilize 3D nano/microfabrication approaches in order to create biomimetic models of the ECM from these images. These models can then be manipulated to study the signaling pathways associated with cancer. Additionally, the models can provide insight into the design of tissue engineering scaffolds.

During synthesis of the ECM model, a solution of a particular protein and the Rose Bengal photoactivator are pipetted into a hybridization chamber attached to a glass slide. The protein solution used for the reaction can vary-- either Fibronectin, Laminin 1 (alpha 1, beta 1, gamma 1) or Collagen type 1 -- while the concentration of that particular protein solution ranges from 15-24% of stock protein. The glass slide apparatus is then placed underneath the laser setup within a microscope’s working platform. Then, a titanium sapphire laser operating at 780 nm for 100 femtoseconds induces a two-photon excitation of the Rose Bengal photoactivator [1]. This leads to a series of photochemical reactions that result in the generation of a radical of the particular protein, which links to a second protein radical in solution and generates a covalent bond. Currently, this process is then repeated over 3 hours in order to generate a full ECM scaffold. From this process, the ECM scaffold can then be studied to gain knowledge that can ultimately be implemented into the clinical field.

Problem Statement

Dr. Campagnola's lab has designed and constructed several microscope-based instruments for creating 3D nano/microstructure tissue engineered scaffolds. These are used for studying cell-extracellular (ECM) interactions in cancers and fibrosis as well as for general biology applications. Currently, the method of introducing and eliminating excess protein solution is done by hand with a micropipette. This process is tedious and prolongs the fabrication process. Additionally, after the experiment is run, a large majority of the protein solution is disposed of due to possible contamination from ECM particulates that have broken off of the scaffold. Our client seeks an automated system capable of introducing protein solution, filtering excess precipitate, and recovering a majority unpolymerized protein solutions for re-use. This device will be controlled by pumps and ideally integrated into the current LabVIEW framework.

II. Background

Client Information

Dr. Campagnola received his BA in chemistry at Colgate University in 1986 and his PhD in physical chemistry at Yale University in 1992 [2]. His lab focuses on studying the alterations of extracellular matrix (ECM) in epithelial cancers as well as in connective tissue disorders. His lab utilizes Second Harmonic Generation imaging microscopy along with two-photon excited fluorescence for the imaging of structural aspects of tissues. These approaches will ultimately be implemented as clinical diagnostics [2]. Dr. Campagnola's lab also uses 3D nano/microfabrication approaches to create biomimetic models of the ECM to study signaling pathways associated with cancer and provide insight into the design of tissue engineering scaffolds.

Extracellular Matrix Imaging

As mentioned previously, two-photon excited fluorescence and Second Harmonic Generation are utilized to generate high resolution microscopy "slices" of a desired ECM subset. This image data is then processed as an 8-bit grayscale image with respect to the Nyquist criterion, which is an important step in ensuring that the resolution of the image and 3D representation match [1]. This step is also crucial in ensuring the 3D structural integrity of the generated ECM scaffold and to guarantee the scaffold is an accurate representation of the tissue. The image is then further processed utilizing ImageJ in order to generate patterns which eliminate the imaging static created by the overlapping fibers of the ECM [1]. This allows for the optimally desired structural pattern for replication to be discerned from the imaging data.

Modulated Raster Scanning

During synthesis, a solution of a particular protein of the ECM and the Rose Bengal photoactivator are pipetted onto a microscope slide underneath the laser apparatus (Figure 1). The solution protein varies -- either Fibronectin, Laminin 1 (alpha 1, beta 1, gamma 1) or Collagen type 1 -- while the concentration of each particular stock protein is initially 1mg/mL it is diluted to 200mL, at a concentration of 15-24% stock protein. Amount of protein being used per trial depends on the structure being created, but can be estimated by using the volume of a "block". The x and y direction lengths of the block are 2400 microns, while the z direction lengths varies, ranging from 3 to 50 microns. The volume of solution per trial ranges from 45 - 50 μ L, with around 35 μ L of that solution being excreted as waste from the system. Then, the titanium sapphire laser operating at 780 nm for 100 femtoseconds induces two-photon excitation

of the Rose Bengal photoactivator [1]. The short pulse width of the laser is essential in fully inducing two-photon absorption of the photoactivator and ensuring precise fabrication of the scaffold [3]. Further, that same short pulse width allows the laser to operate at a constant peak power density while not causing any side reactions or denaturing the proteins [4]. This leads to a series of photochemistry reactions that result in the generation of a radical of the particular protein, which links to a second protein radical in solution and generates a covalent bond [5]. Using their current methods, this process is then repeated over 3 hours in order to generate layered slices of the desired ECM scaffold, which then can be synthesized into a full ECM scaffold [1-4].

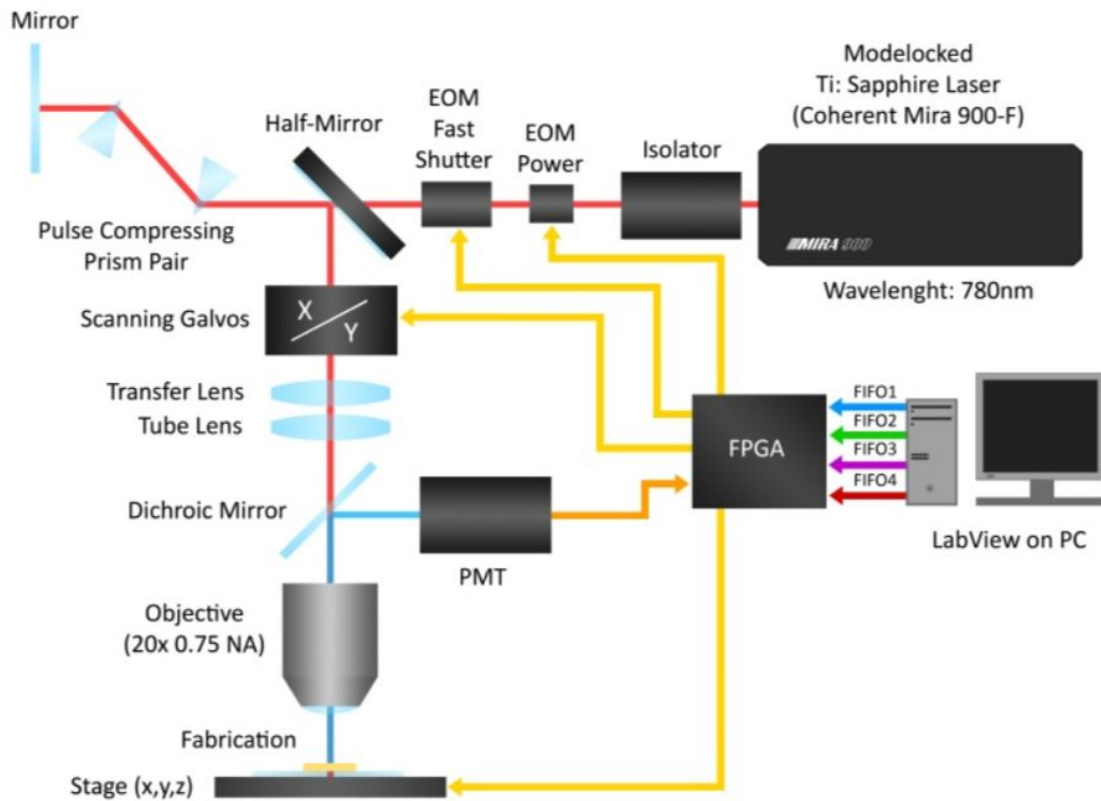


Figure 1: Computer generated representation of the specific laser apparatus [1].

The specific laser microscope apparatus is set up to modulate the power output of the laser with the slow electro-optic modulator (EOM) before it enters the fast shuttering EOM. This permits constant peak power output to be utilized during the scanning process [1]. Consequently, since the fractional dwell for each pixel linearly defines the integrated exposure dose of the ECM proteins, it is possible to linearly correlate the intensity of contrast in the generated grayscale image and the resulting protein concentration of the scanned ECM subset [1]. By relating the protein monomer crosslinking speed to the protein concentration when fabrication conditions are kept under the same power density and when exceeding the overall power threshold [6-7], it is

possible to manually synthesize an ECM scaffold based on a processed scan of a subset of the ECM. Furthermore, an ECM subset that was synthesized utilizing the processes described above had a 96% fidelity between itself and the original ECM scan. This percentage was obtained using pixel by pixel co-localization testing in ImageJ [1].

Summary of Product Design Specifications

The client seeks:

- A microfluidic device capable of washing and recollecting proteins
 - Proteins used as collagen, laminin, and fibronectin
 - Volume of protein used ranges from 10 μL to 100 μL
- Four compartments that can be used at the same time
 - Fourth compartment is for PBS solution
- Easy integration into LabView
 - A program already used in Dr. Campagnola's lab
- The ability to filter out any ECM particulates 200 μm and smaller
 - Protein solutions must maintain concentration range of 15-24%
 - Collected at greater than 70% of the original sample of proteins
- The filters being used must be easy to clean or not costly to replace
- Materials being used must be resistant to protein adsorption
 - Must be inert as well to not interfere with the laser
- The product to be within a 1500\$ budget

Summary of Previous Semester's Work

Last semester, the team designed a microfluidic device that would pump protein solution into a reaction chamber and then filter the solution as it exited the device. The team created two design matrices to decide the best approach to two aspects of the microfluidic apparatus. First, the team decided how to input the protein solution into the device. After careful consideration of two proposed designs, the team decided that a pressurized capsule would most effectively transport the protein solution into the reaction chamber. The premise of this input design was to incorporate a pressurized pump that will connect directly to several capsules. The majority of the capsules contained the individual protein solutions with their photoactivator while one capsule contained the solution for washing out the well. Ideally, the capsules would have a threaded cap that will allow the user to easily insert the solutions via micropipette. Upon adequate pressure induced by the pump into the capsule, the solution would flow out of the capsule and pass through a bubble detector (as detrimental effects will occur if there is sufficient air within the well and the client attempts to polymerize the protein solution) and subsequently into the well. Ideally, one could control the pump and obtain information from the bubble detector using

Labview software. By the end of the semester, the team assembled the pump, the necessary tubing, and the microfluidic device chamber. Due to issues controlling the pump, the team could not test the prototype, and the bubble detector was too expensive for the given budget.

Secondly, the team explored options for filtering the protein solution to remove pieces of ECM that fall off the scaffold. The design that the team chose incorporated a thin slide with a circular filter opening within it to filter precipitate out of the protein solution downstream of the reaction chamber. This design included a gap in the structure for the slide to move across so that the slide can line up the opening with individual output channels. The filter within the slide apparatus would be removable via an insert similar to that of a SIM card tray of a phone, permitting simple filter replacement. Despite having a relatively simple method of filtering out the precipitate from the protein solution, the production of the slide apparatus would be difficult due to the scale that the piece would have to be built to (especially with the inner removable tray that would house the filter). On these grounds, the team never pursued fabrication of this device but rather bought a filter that could attach to the output tubing. The team has since reconsidered these options, since including the filter as part of the microfluidic system makes the device prone to clogging and developing back pressure that could harm the pump.

The final proposed design (Figure 2) included both of the above components. Due to the scale of the device, the team contracted Midwest Prototyping to 3D print the microfluidic reaction chambers. They printed two devices out of different nonfouling materials with plans to test which adsorbed less protein at the end of the semester. The team purchased tubes made of polytetrafluoroethylene and a piezoelectric pump.

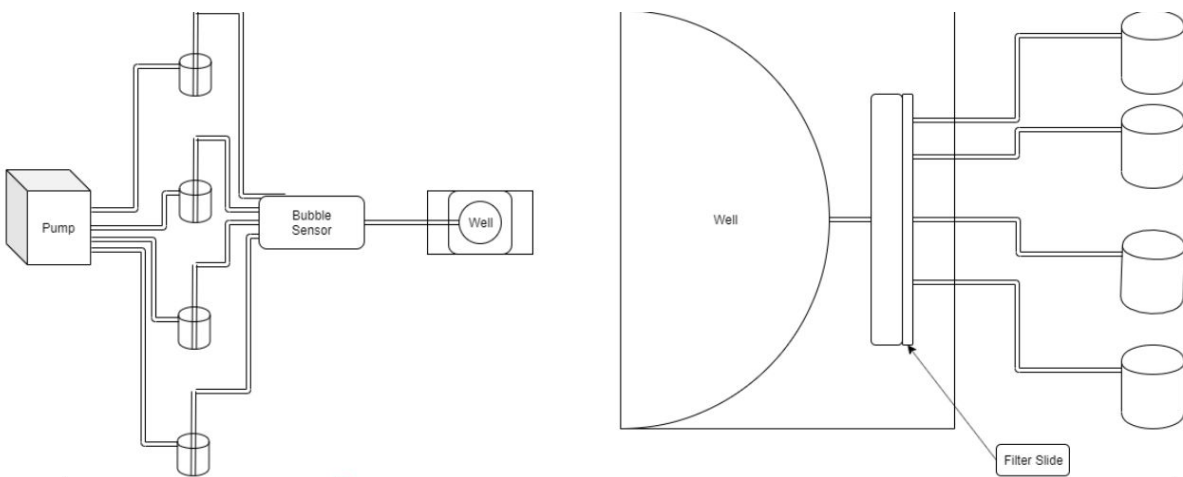


Figure 2: Combination of pressurized capsule input and slider filtration output for final design from last semester.

Two different designs for the microfluidic device, the weighted and clip designs, were created in SolidWorks to house the proteins during ECM synthesis. These designs both incorporate an input port, the well, and an output port. The input port is where the proteins will

be fed towards the well to be synthesized. From here, the excess proteins and precipitate can be filtered out of the output port. Both of these designs also need to have a tight seal in order to maintain pressure. On top of both is a slot for a cover slip to rest over the well area. The two designs were also fabricated from two different materials, SIL-30 [8] and EPU-40 [9].

Weighted

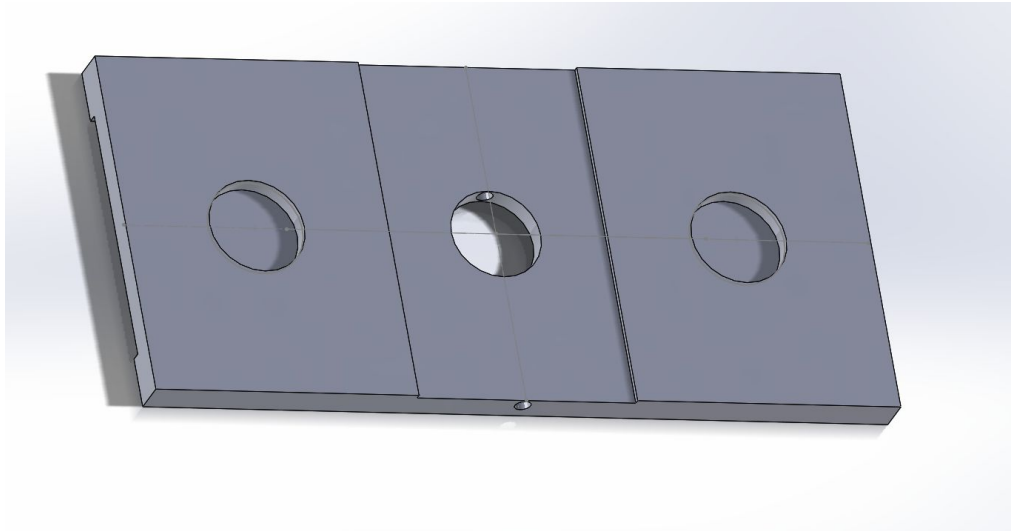


Figure 3: SolidWorks design for weighted method, top view.

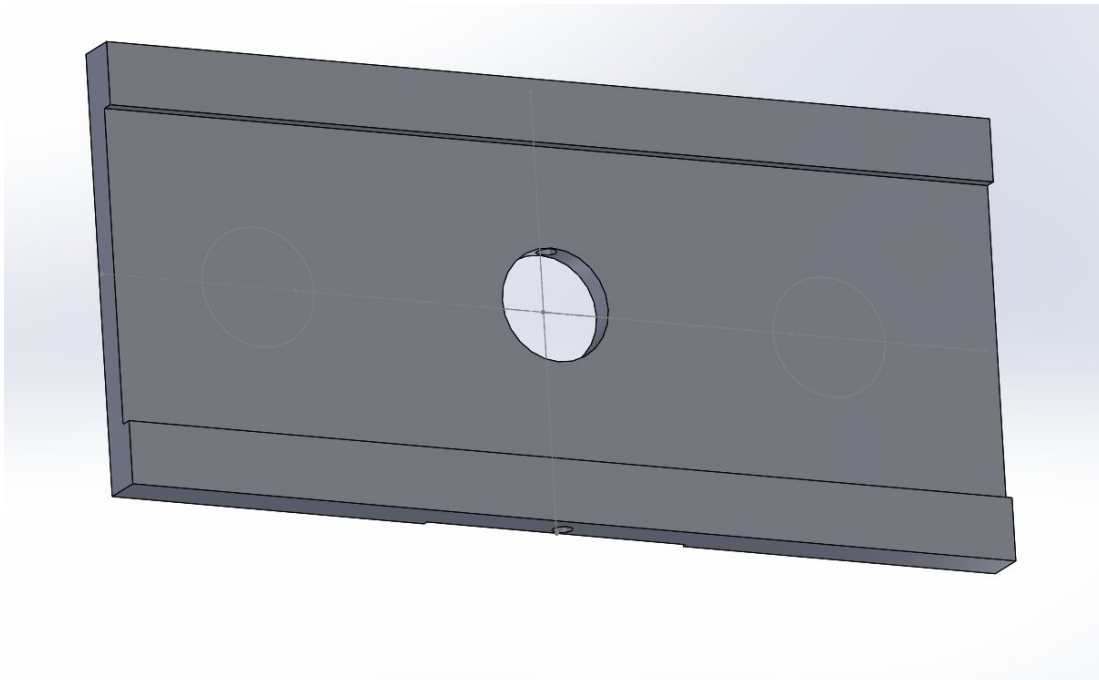


Figure 4: SolidWorks design for weighted method, bottom view.

The weighted 3D well design uses gravity and physical weights to sandwich each component together in order to maintain a tight seal. The bottom incorporates the entire glass slide for ECM synthesis. On top are two slots for round weights. This will make sure the device is pressing on the glass slide with enough force to maintain a tight seal and pressure. Round holes for input and output are taken out to make room for the PTFE tubing towards the well.

Clip

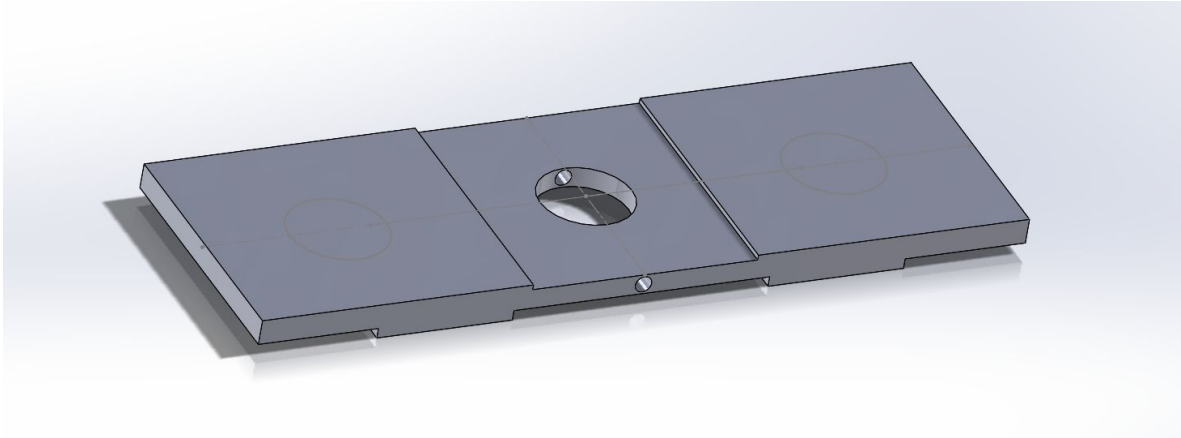


Figure 5: SolidWorks design for clip method, top view.

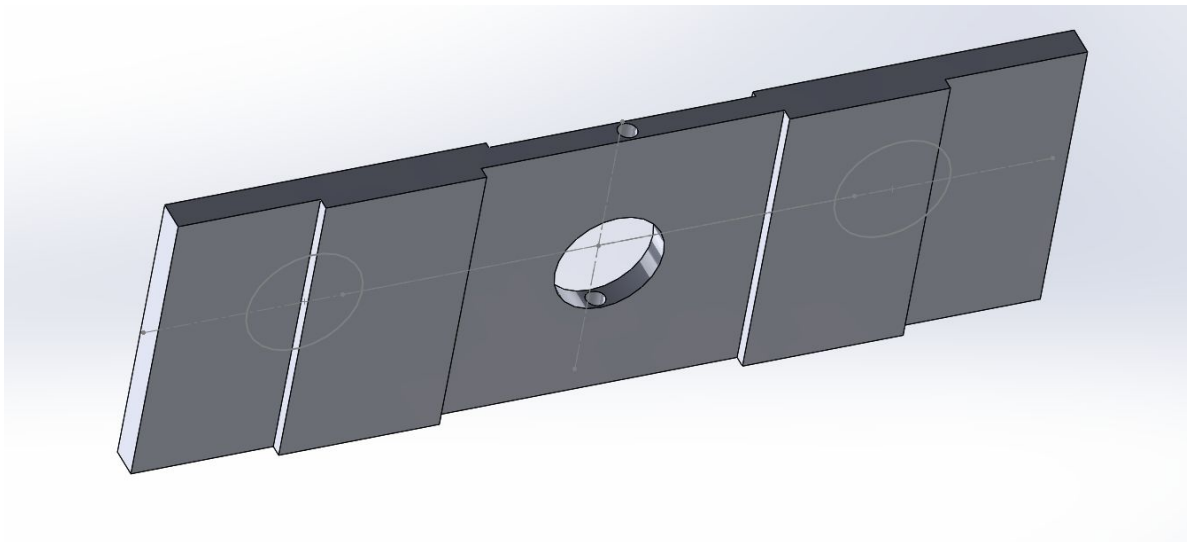


Figure 6: SolidWorks design for clip method, bottom view.

The clip design works in a similar fashion to the weighted design, as a tight seal needs to be maintained throughout. The bottom has a slot for a smaller lengthwise-cut glass slide. There are also two extended portions of the device where a clip can be attached. This clip will press the shortened glass slide up into the device in order to maintain a tight seal and pressure.

III. Preliminary Designs

Weights

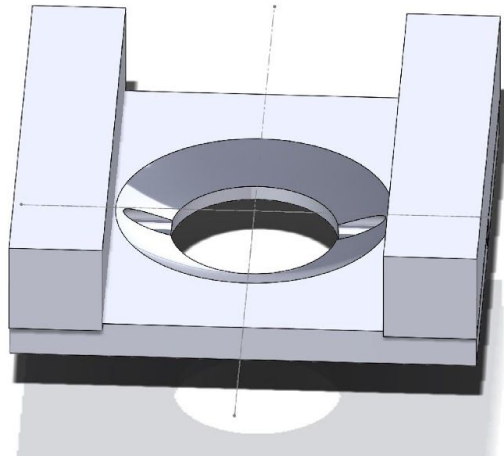


Figure 7: SolidWorks design for the weight design

The weights design uses simple weights to seal the hybridization chamber. The weights will be in the shape of rectangles, to seal the hybridization chamber. The weights can be placed at multiple different places, allowing this design to be amended for the best possible seal to occur. The weights would be placed on top of the glass slide, and by their weight, would hold down the glass slide.

Clamp

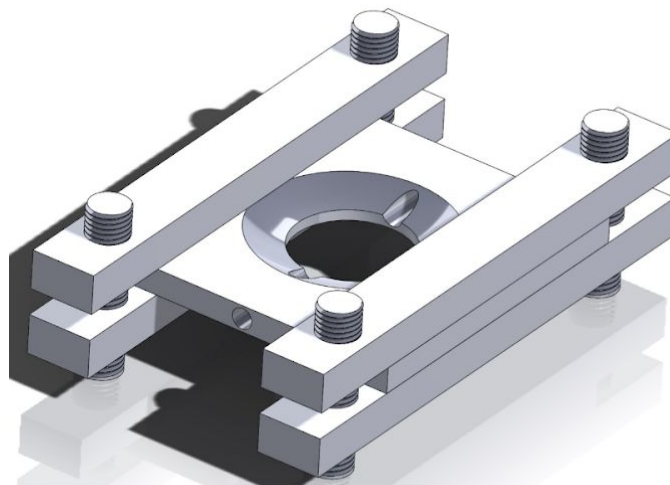


Figure 8: SolidWorks design for the clamp design

The clamp design incorporates the same size hybridization chamber as does the others. The method for maintaining a tight seal uses two sets of clamps to hold and sandwich together all components. These clamps would be manually tightened with a screw in order to keep all of the parts in place.

Magnets

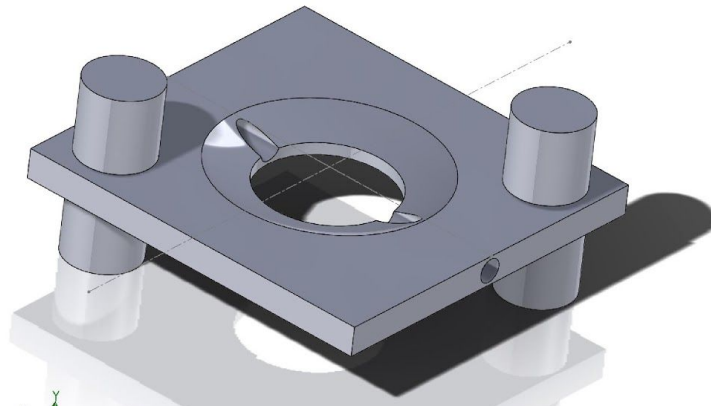


Figure 9: SolidWorks design for the magnet design

The magnet design deploys two oppositely charged magnets being placed above and below the glass slide of the hybridization chamber. When this is done, the chamber would be effectively sealed. The magnets can also be moved to different corners of the glass slide to whichever combination that provides the best seal. More magnets can also be used on this design if two magnets are determined to not be enough.

IV. Preliminary Design Evaluation

Design Matrices Summary

As part of the selection process, a design matrix was created to assess the designs based on several criteria. Five selected categories were chosen and arranged for the design matrix with the most important at the top and the least important at the bottom. Each criterion was given a fixed score that when totaled up equals 100. The team has created a design matrix that assesses the three designs for sealing the hybridization chamber.

Five different categories were assessed for these three designs. Ease of fabrication was the highest weighing at thirty-five percent. If the component is too difficult to create, then the design would be useless. Sealing capabilities was next weighing twenty-five percent. In order for protein solution to flow in and out of the chamber, a tight seal should be met. Ease of use is weighed next at twenty percent. This refers to how each design would be operated, considering

both time and amount of labor for the user. Cost weighs fifteen percent. This category refers to how much money each component would be to purchase. The final criterium is durability at five percent. Durability takes into account how long each design could last over repeated uses.

Design Matrix

Table 1: A design matrix comparing methods of maintaining a tight seal at the coverslip-EPU-40 interface.

Weight	Criteria	Weights		Clamp		Magnets	
35	Ease of Fabrication	4	28	4	28	4	28
25	Sealing Capabilities	1	5	5	25	3	15
20	Ease of Use	4	16	3	12	4	16
15	Cost	4	12	4	12	3	9
5	Durability	5	5	5	5	5	5
100	Total (100)	66		81		74	

Weights

The weights design scored the lowest of all three at sixty-six. It was given a four for its ease of fabrication, since no additional components need to be made within the solidworks design. Its sealing capabilities were given a one. These weights would not be very secure on top and could shift during the process. This could cause the seal to break and have a loss of pressure. Ease of use was given a four as it would be simple to operate. The weights only need to be placed on top of the cover slip. Cost was also given a four as weights are fairly inexpensive. Lastly, durability was given a five, since the weights would have minimal wear and tear over multiple uses.

Clamp

The clamp designed received the highest score of the three designs with a score of eighty-one. The ease of fabrication of the clamp design received a score of four. It was a high score because only two pieces of material with threaded holes and threaded rods would be needed. Once these materials are found, they just need to be put together. The clamp received the highest score of five for sealing capabilities because the seal is adjustable, allowing for the tightest possible seal possible during any experiment. The ease of use for the clamp received a

score of three because this design requires physically moving a mechanism, something not found in the other designs. This design received a high score of four for cost because all the materials can be found in the engineering buildings on campus. No excess material would need to be purchased for the clamp design. Finally, a score of five was given to the clamp design for durability because it is a simple design with only two moving parts.

Magnets

The magnets design received the second highest score with a score of seventy-four. The design received a score of four for ease of fabrication because the design only includes magnets. No other materials are needed for this design, allowing for simple and quick fabrication. Next, the design scored a score of three for sealing capability because if the magnets are not placed in the correct spots there is a possibility of airflow reaching the hybridization chamber. An advantage to the magnets is the ease of use. The magnets received a score of four because in order for the magnets to seal the chamber, the two oppositely charged magnets just have to be placed on top and bottom. A disadvantage of the magnets is the cost compared to the other designs. Effective magnets would need to be purchased for this design to work. Due to this the magnet design received a low score of three for the cost category. Finally, magnets received a high score of five for durability because magnets are extremely durable and hard to break.

V. Fabrication/Development Process

Materials

This device will be used with proteins such as fibronectin, laminin and collagen, so the materials need to resist adsorption. The tubing used to transport the proteins is made of polytetrafluoroethylene (PTFE) which resists adsorption of proteins due to having very hydrophobic properties [10]. The 3D well designs will also be in direct contact with the proteins, so their surfaces need to reduce adsorption as well. Two different materials were under consideration; those being silicon (SIL) 30 and elastomeric polytetraurethane (EPU) 40. SIL-30 is a 3D printing material that has biocompatibility, low durometer, and tear-resistance [8]. EPU-40 is also a 3D printing material that has high elongation and tear strength [9]. According to Midwest Prototyping, both of these materials are used in biomedical applications, but the company was not able to provide information about the hydrophobicity/adsorption properties of the two materials. Testing was done on the materials, and neither had an advantage over the other for protein adsorption. See testing and results for further analysis. The team chose EPU-40 as the main material to be used due to its rigidity.

Final Design

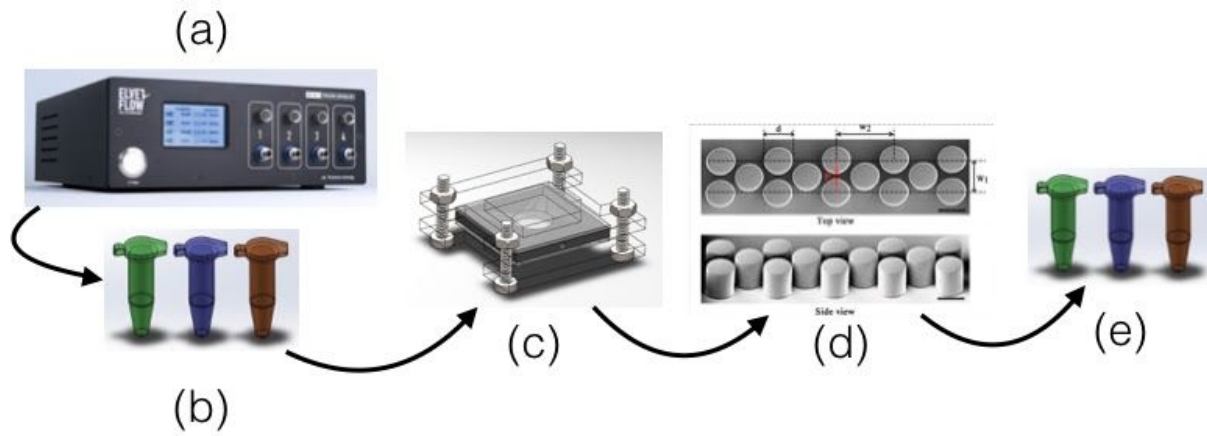


Figure 10: Full assembly of system a) OB1 controller b) inlet tubes c) clamp d) pillar filters e) outlet tubes

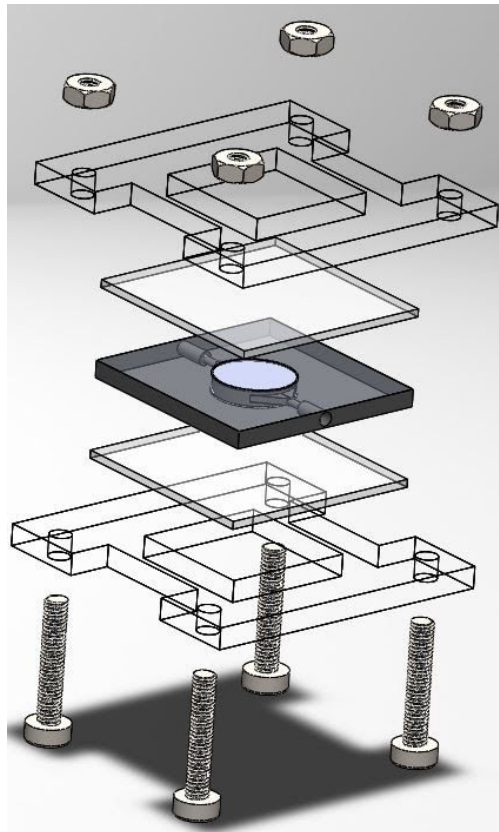


Figure 11: Assembly view version of microfluidic device

Figure 10 depicts the full assembly that the team proposes. To connect each segment, PTFE tubing will be used. Starting with (a), the OB1 multi-channel microfluidic flow controller[11] exerts pressure into individual capsules (b) that contain the separate protein solutions or cleaning agent. Upon optimal pressure induced, the solution will flow out of the capsule and into the microfluidic device (Figure 11 depicts an easier interpretation of the device by showing the individual components holding the microfluidic device to the microscope glass slides). After the client conducts the ECM synthesis, the OB1 pump will continue to push unsynthesized solution through a built-in filtering mechanism in the microfluidic device (d). The idea behind this mechanism is that the pillars[12] allow broken pieces of ECM scaffold to be captured while permitting the rest of the unpolymerized solution to pass through and be collected in individual capsules (e).

VI. Testing & Results

Testing Protein Adsorption

The purpose of this test was to see if proteins adsorb to the material when exposed to a protein solution over a long period of time. By minimizing the protein adsorption onto the material, the recovery of the proteins will be maximized. In this test, EPU-40 and SIL-30 were individually placed in separate dishes filled with Bovine Serum Albumin (BSA). By using a spectrophotometer set to a wavelength of 280 nm [13], the optical density (OD) of 3 samples of BSA in a petri dish with either material were gathered in intervals of 5 minutes, 10 minutes, 30 minutes, 60 minutes, 120 minutes, and 180 minutes. As a control, regular BSA was by itself in a separate petri dish. The OD shows the relative degree to which a refractive medium retards rays of light. This measure is useful because the material with the higher optical density is also the material with the least amount protein adsorbed to it.

Average Optical Density of SIL 30, EPU 40, and Control Over Time

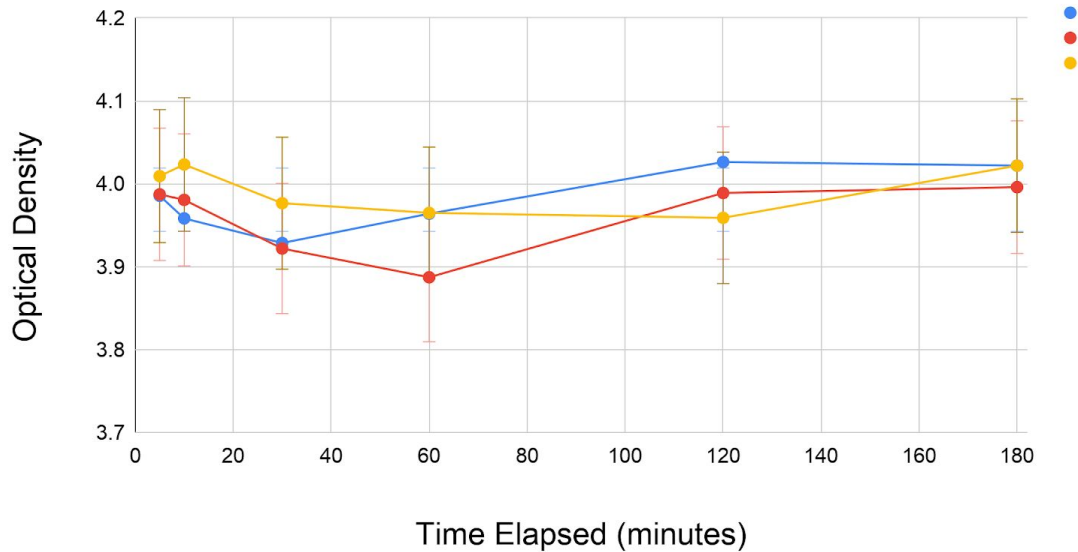


Figure 12: Graph of the average optical density of SIL 30 (blue), EPU 40 (red), and control (yellow) over time

An average was taken on each sample's OD at their respective time points. The average values were all similar and the standard deviation and variance were calculated to display the average distance away from the mean. A couple of T tests were computed with an α -value of 0.05. In the test between the control and SIL 30, a p-value of 0.6984 was computed. In the test between the control and EPU 40, a p-value of 0.1743 was determined. In comparing between the two biomaterials, a p-value of 0.3361 was computed.

Velocity and Pressure Profile Inside Tubing

In order to derive the velocity and pressure profile of the solution inside the tubing, the Navier-Stokes equation of momentum transport was used. In order to simplify the equation, assumptions regarding the solution and the environment were made. The first assumption was that the velocity profile in the z direction, or down the tube, depended only on the r, or radial direction of the tube. In addition, the environment was assumed to be a steady state environment and that the solution has a constant density and viscosity. Finally, the effects of gravity were considered to be zero.

$$\rho \frac{D}{Dt} \mathbf{v} = -\nabla p + \mu \nabla^2 \mathbf{v} + \rho \mathbf{g}$$

Equation 1: The Navier Stokes equation

$$\rho \left(\frac{\partial v_z}{\partial t} + v_r \frac{\partial v_z}{\partial r} + \frac{v_\theta}{r} \frac{\partial v_z}{\partial \theta} + v_z \frac{\partial v_z}{\partial z} \right) = -\frac{\partial p}{\partial z} + \mu \left[\frac{1}{r} \frac{\partial}{\partial r} \left(r \frac{\partial v_z}{\partial r} \right) + \frac{1}{r^2} \frac{\partial^2 v_z}{\partial \theta^2} + \frac{\partial^2 v_z}{\partial z^2} \right] + \rho g_z$$

Equation 2: Equation of motion for Newtonian Fluid with constant density and viscosity in the z direction

Once these terms of the equation were eliminated, the equation was integrated twice, and the constants were solved for using boundary conditions seen in Appendix C. Once the constants were solved for, the velocity and pressure profiles were fully derived. In order to solve for the volumetric flow rate (Q), which is the amount of fluid passing in the tube per unit time, the velocity profile was integrated with respect to the z and θ directions. Full calculations can be seen in Appendix C.

$$v_z(r) = \frac{(p_0 - p_L)R^2}{4\mu L} \left(1 - \left(\frac{r}{R}\right)^2\right)$$

Equation 3: Velocity profile for inside the tube.

$$p(z) = p_0 - (p_0 - p_L)\left(\frac{z}{L}\right)$$

Equation 4: Pressure profile for inside the tube

$$Q = \frac{\pi(p_0 - p_L)R^4}{8\mu L}$$

Equation 5: Volumetric Flow rate of the liquid inside the tube

Simulation of Pressure in Microfluidic Device

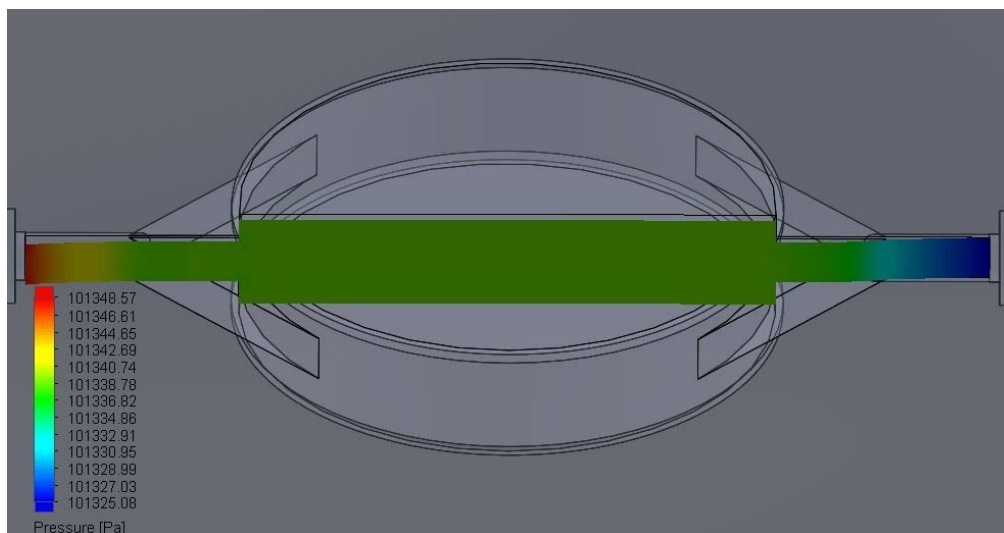


Figure 13: SolidWorks pressure simulation inside microfluidic chamber

The pressure flow simulation shows pressure distribution inside the fabricated microfluidic device. The inlet hole of the device, on the left, has the greatest pressure because the pump will be pressurizing the tube at the beginning of the tubing. The outlet hole, on the right side of the image, will have the least amount of pressure because the majority of the pressure is dissipated within the microfluidic device. The center of the microfluidic device, where the reaction will take place, is at a constant pressure throughout. This shows that there are no high pressure areas inside the device that would cause leaking to occur.

VII. Discussion

Protein Adsorption Test

Using an α -value of 0.05, the tests showed that there was no significant difference between the average OD's of EPU 40 and SIL 30. There also was no significant change in OD when comparing the individual materials to the control. From these two core pieces of information, it was deduced that despite having protein adsorption, there is no statistical advantage to using one biomaterial over the other. Qualitatively speaking, there was protein adsorption to both materials. This was clearly evident from the same experiment last semester when the team used a solution of BSA with a photoinitiator that resulted in a red tint to the materials. Despite the lack of significance, the team has elected usage of EPU 40 due to the fact that it is much more rigid than SIL 30.

Future Work

- Contact Midwest Prototype to fabricate the new design
 - Currently, EPU-40 will be used as the material
- Discuss with client the possibility of purchasing a controller
 - Elveflow package including OB1 controller/pump and other attachments needed costs 5,400 euros
 - This would put the project over budget
- Fix fabricated clamp
 - Find screws that are the correct length to close the clamp
- Begin physical tests
 - Luminescence tests
 - Soak SIL-30, EPU-40, and a control for set amount of time
 - View with electron microscope
 - Compare brightness on ImageJ
 - Flow rate tests

- Pump set amount liquid through tubing using programmed microcontroller
- Time how long it takes for liquid to exit tubing
- Adjust microcontroller to desired flow rate
- Clamp sealing capabilities
 - Clamp the microfluidic device together and fill with water
 - Observe to see if water leaks out the edges
- Assemble entire system
- Integration with LabView software

VIII. Conclusion

The client, Dr. Paul Campagnola, has proposed a fully automated system to allow transport of protein solutions in and out of a well to be developed. This would allow for an easier fabrication process of ECM synthesis while reducing production time. Continuing on the work that was done in the last semester, a new design was determined for the microfluidic device while the whole system itself retains the basic inflow premise. It is recommended that the client purchases the OB1 multichannel pump as it is compatible with LabView software and can be used for multiple applications. Likewise, the microfluidic device should be outsourced for 3D printing with minimal extra manufacturing needing to be done. Ultimately, the team exerts confidence that the system will work based on theoretical analysis but should still be tested in-field if further modifications to the design need to be made.

IX. References

- [1] V. Ajeti, C. Lien, S. Chen, P. Su, J. Squirrell, K. Molinarolo, G. Lyons, K. Eliceiri, B. Ogle, and P. Campagnola, "Image-inspired 3D multiphoton excited fabrication of extracellular matrix structures by modulated raster scanning", *Optics Express*, vol. 21, issue 21, pp. 25346-25355, 2013.
- [2] P. Campagnola, "Profile Summary", College of Engineering University of Wisconsin - Madison, Accessed on: Nov. 2019, Available: https://directory.engr.wisc.edu/bme/Faculty/Campagnola_Paul/.
- [3] C. Lien, W. Kuo, K. Cho, C. Lin, Y. Su, L. Huang, P. Campagnola, C. Dong, and S. Chen, "Fabrication of gold nanorods-doped, bovine serum albumin microstructures via multiphoton excited photochemistry", *Optics Express*, vol. 19, issue 7, pp. 6260-6268, 2011.
- [4] L. Cunningham, M. Veilleux, and P. Campagnola, "Freeform multiphoton excited microfabrication for biological applications using a rapid prototyping CAD-based approach," *Optics Express*, vol. 14, issue 19, pp. 8613-8621, 2006.
- [5] Y. Sie, Y. Li, N. Chang, P. Campagnola, and S. Chen, "Fabrication of three-dimensional multi-protein microstructures for cell migration and adhesion enhancement", *Biomedical Optical Express*, vol. 6, issue 2, pp. 480-490, 2015.
- [6] J.L. Boulnois, "Photophysical processes in recent medical laser developments: A review", *Laser in Medical Science*, vol. 1, issue 1, pp. 47-66, Jan. 1986.
- [7] S. Basu, C. Wolgemuth, and P. Campagnola, "Measurement of normal and anomalous diffusion of dyes within protein structures fabricated via multi-photon excited crosslinking", *Biomacromolecules*, vol. 5, issue 6, pp. 2347-2357, Sept. 2004.
- [8] "Silicone (SIL) 3D Printer Material," Carbon. [Online]. Available: <https://www.carbon3d.com/materials/silicone/>.
- [9] "Elastomeric Polyurethane (EPU) 3D Printer Material," Carbon. [Online]. Available: <https://www.carbon3d.com/materials/epu-elastomeric-polyurethane/>.
- [10] R. Freitas, 15.3.4.1, 2003. [Online]. Available: <http://www.nanomedicine.com/NMIIA/15.3.4.1.htm>. [Accessed: 10-Dec-2019].
- [11] "OB1 - 4 channels microfluidic Flow controller," Elveflow. [Online]. Available: <https://www.elveflow.com/microfluidic-products/microfluidics-flow-control-systems/ob1-pressure-controller/>. [Accessed: 27-Mar-2020].
- [12] I. Biswas, A. Kumar, and M. Sadrzadeh, "Microfluidic Membrane Filtration Systems to Study Biofouling," *Microfluidics and Nanofluidics*, Feb. 2018.
- [13] A. Seifert, "Characterization of bovine serum albumin/ chlorogenic acid solution mixtures by analytical ultracentrifugation," *University of Nottingham*, 2004. [Online]. Available: <https://www.nottingham.ac.uk/ncmh/documents/papers/paper282.pdf>. [Accessed: 23-Feb-2020].

X. Appendices

Appendix A: Product Design Specification (PDS)

Microfluidic Device

Preliminary Product Design Specifications

Team: Jason Wang
Robert Meuler
Jiacoimo Beckman
Nick Pauly
Kevin Koesser

Date: Friday February 7, 2020

Function:

The client's lab has designed and constructed several microscope-based instruments for creating 3D nano/microstructure tissue engineered scaffolds. This instrument includes rapid laser shuttering at 10 MHz [1] that results in a network of polymerized protein concentrations that are reflective of grayscale image data. The resulting scaffolds are used for studying cell-extracellular (ECM) interactions in cancers and fibrosis as well as for general biology applications.

Currently, the client's lab procedure for producing these scaffolds is very inefficient in protein usage and human labor. Therefore, our client seeks a microfluidic device capable of washing out the unpolymerized proteins of low volumes ranging between 10 μL to 100 μL . These expensive proteins include collagen, laminin, and fibronectin and should be recollected for re-use. This device will allow a decrease in production time for the engineered scaffolds and decrease cost associated with the experiments. If the device is effectively implemented, it will be used in the client's future research projects.

Client Requirements:

- Compartment(s) that house water and protein solutions such as collagen, laminin, and fibronectin.
- These protein solutions should be filtered and collected separately to be reused in future trials
- Must be compatible with LabVIEW software.
- Must maximize the recovery of the major proteins- fibronectin and laminin take precedence.
- Can be used for other projects.

- Combined budget: \$1,500

Design Requirements:

- *Performance Requirements*
 - Maximize the percentage of material recovered.
 - Used over a maximum of 3 hours
 - Reusable for multiple procedures.
 - Parts must be easily interchangeable from wear and tear.
 - Resists protein adsorption over the length of the procedure
 - Needs to withstand the power density of the laser ($\sim 1.0 \times 10^{17}$ (W/cm²)) [2].
 - Needs to be compatible with existing LabVIEW framework.
- *Safety*
 - Materials used should be able to withstand the laser without decomposing or affecting the culture.
 - Materials should be compatible with the requirements listed for Biosafety level 2 lab
 - No exotic materials with a risk of causing aerosol-transmitted infections [3]
 - Should not give out an excessive amount of heat that would damage the ECM as well as give off too much light that could affect any experiments.
 - No visible circuitry or moving parts that would affect the user or any other components of the experiment.
- *Accuracy and Reliability*
 - Should recollect greater than 70% of the original sample of proteins
 - Original sample: 45 - 50 μ L of solution
 - Concentration of proteins in solution range from 15 - 24%
 - Proteins recovered should be in the same concentration as the original sample
- *Life and Service*
 - Used for 3 hours at a time, on average
 - Used daily
- *Shelf Life*
 - Shelf life should be at least a year
- *Operating Environment*
 - Biosafety Level 2
 - Withstand power density of laser ($\sim 1.0 \times 10^{17}$ (W/cm²))
 - No light emission
- *Ergonomics*
 - Used in a controlled laboratory environment (biosafety level 2)
 - Operated by professionals through LabVIEW software

- *Size*
 - Smaller than a regular microscope slide with thickness of 1 mm
 - Similar size to current hybridization chamber currently used in procedure
 - Contain up to 50 μL
- *Weight*
 - Should not exceed .25 kg, which could potentially damage lab microscope
- *Materials*
 - Use materials that are as inert as possible to the conditions of the laser
 - The material should not attract and adsorb proteins.
 - Tests will be done to determine adsorption of BSA by the materials
 - Tentative materials include SIL-30 and EPU-40 [4]
- *Aesthetics, Appearance, and Finish*
 - Aesthetic must not affect the capabilities of the laser or any other component.
 - Concealed and clean finish

Production Characteristics:

- *Quantity: 1 design*
- *Target Production Cost: less than \$1500*
 - Total budget includes purchases made in Fall 2019 semester

Miscellaneous:

- *Standards and Specifications*
 - No human subjects are required for this project, therefore no IRB regulations are required in particular to this assignment.
- *Patient Related Concerns*
 - There are no patients or research subjects that will be directly interacting with this device during use.
- *Competition*
 - Currently, there does not exist a product in the market that exactly meets the needs of our client. There are several components that do exist, such as a microfluidic device powered by a pump [5]. Another component to consider is the microfluidic pump itself [6].

Literature Cited

- [1] Ajeti, V., Lien, C., Chen, S., Su, P., Squirrell, J., Molinarolo, K., Lyons, G., Eliceiri, K., Ogle, B. and Campagnola, P. (2013). *Image-inspired 3D multiphoton excited fabrication of extracellular matrix structures by modulated raster scanning*. The Optical Society.
- [2] Sie, Y., Li, Y., Chang, N., Campagnola, P. and Chen, S. (2015). *Fabrication of three-dimensional multi-protein microstructures for cell migration and adhesion enhancement*. The Optical Society.
- [3] “CDC LC Quick Learn: Recognize the Four Biosafety Levels.” *Centers for Disease Control and Prevention*, Centers for Disease Control and Prevention, www.cdc.gov/training/QuickLearns/biosafety/.
- [4]Midwestproto.com. (n.d.). *CLIP Materials @ Midwest Prototyping Additive Manufacturing*. [online] Available at: <https://www.midwestproto.com/technologies/CLIP-Materials> [Accessed 6 Oct. 2019].
- [5] Beebe, D. J., & Walker, G. M. (2002). *Method of pumping fluid through a microfluidic device*. Wisconsin Alumni Research Foundation.
- [6] Young, L. C., & Zhou, P. (2004). *Microfluidic pump and valve structures and fabrication methods*. Rheonix Inc.

Appendix B: Expenses and Purchases

Note: All of these purchases were made in Fall 2019

Item	Description	Manufacturer	Part Number	Date	QTY	Cost Each	Total	Link
Category 1 - Items Purchased By Client								
PTFE Tubing 1/16" OD x 1/32" ID (20 m)	Teflon tubing	Darwin Microfluidics	n/a	11/1/2019	1	\$60.30	\$60.30	LINK
Upchurch Precolumn MicroFilter	PEEK housing with in-line filter connects capillary tubing (using Microtight tubing sleeves) or 1/16 in. O.D. tubing to female 10-32 fitting. Swept volume of 0.3 µL. Includes 5 × 0.5 µm frits (one installed).	Sigma Aldrich	502685	11/11/2019	1	\$128.00	\$128.00	LINK
Piezoelectric Pump	The Piezoelectric Pump is a thin, compact, and lightweight diaphragm micro-pump which has been specifically designed for space-conscious built-in applications.	Dolomite Microfluidics	3200138	11/11/2019	1	\$340.00	\$340.00	LINK
Microfluidic Reservoir	This versatile autoclavable microfluidic adapter allows the use of (included) XS Eppendorf	Darwin Microfluidics	n/a	11/11/2019	1	\$130.00	\$130.00	LINK

	tubes (1.5 mL) in microfluidic systems using standard 1/4"-28 fittings interfaced with any pressure source. The adapter is easily installable, autoclavable, and infinitely reusable.							
Pine Car Derby Round Weights, 1-Ounce, 3-Pack	Simple magnetic weights		P350	12/2/2019	1	\$5.48	\$5.48	LINK
Custom 3D Printed Microfluidic Devices	These parts were 3D printed by Midwest Prototype using EPU40 and silicone	Midwest Prototype	n/a	11/20/2019	1	\$52.00	\$52.00	n/a
Category 2 - Items Purchased Out of Pocket								
Poster print	Final poster print for end of semester		n/a	12/5/2019	1	\$48.00	\$48.00	n/a
Poster tube	Poster tube for final poster		n/a	12/5/2019	1	\$3.10	\$3.10	n/a
						TOTAL:	\$766.88	

Appendix C: Mathematical Derivation

Assumptions

- 1) s.s.
- 2) $v_r = v_\theta = 0$
- 3) $v_z = v_z(r)$
- 4) $g = 0$
- 5) constant ρ, μ

$$\rho \left(\overset{3}{\frac{dv_z}{dt}} + \overset{2}{v_r} \frac{dv_z}{dr} + \overset{2}{v_\theta} \frac{dv_z}{d\theta} + \overset{3}{v_z} \frac{dv_z}{dz} \right) = \overset{3}{-\frac{dp}{dz}} + \mu \left[\overset{3}{\frac{1}{r}} \frac{d}{dr} \left(r \frac{dv_z}{dr} \right) + \overset{3}{\frac{1}{r^2}} \frac{d^2 v_z}{d\theta^2} + \overset{4}{\frac{d^2 v_z}{dz^2}} \right]$$

$$-\frac{dp}{dz} + \mu \frac{1}{r} \frac{d}{dr} \left(r \frac{dv_z}{dr} \right)$$

$$\mu \frac{1}{r} \frac{d}{dr} \left(r \frac{dv_z}{dr} \right) = C_0 = \rho g / \rho z$$

$$r^2 \frac{d^2 v_z}{dr^2} = C_0 r^2 + C_1$$

$$\frac{d}{dr} \left(r \frac{dv_z}{dr} \right) = \frac{C_0}{\mu} r$$

$$r \frac{dv_z}{dr} = \frac{C_0}{2\mu} r^2 + C_2$$

$$\frac{dv_z}{dr} = \left(\frac{C_0}{2\mu} r + \frac{C_2}{r} \right)$$

$$v_z(r) = \frac{C_0}{4\mu} r^2 + C_2 \ln r + C_3 = \frac{C_0 r^2}{4\mu} + C_3$$

BCs

$$z=0 \quad p=p_0$$

$$z=L \quad p=p_L$$

$$r=R \quad v_z=0$$

$$r=0 \quad v_z=0$$

$$p(z) = p_0 - (p_0 - p_L) \frac{z}{L}$$

$$v_z(r) = \frac{(p_0 - p_L) R^2}{4\mu L} \left[1 - \left(\frac{r}{R} \right)^2 \right]$$

$$Q = \int_0^{2\pi} \int_0^R v_z(r) r dr d\theta = 2\pi \frac{(p_0 - p_L) R^2}{4\mu L} \int_0^R \left[1 - \left(\frac{r}{R} \right)^2 \right] r dr$$

$$\xi = r/R$$

$$= \frac{\pi (p_0 - p_L) R^4}{2\mu L} \int_0^1 (1 - \xi^2) d\xi = \frac{\pi (p_0 - p_L) R^4}{8\mu L}$$

Appendix D: EPU-40 vs SIL-30 Report for Midwest Prototype

Protein Adsorption

An analysis of EPU-40 and SIL-30

Biomedical Engineering Design 301
Department of Biomedical Engineering
University of Wisconsin
February 15, 2020

Team Members:
Jason Wang
Kevin Koesser
Nicholas Pauly
Jiacomo Beckman
Bob Mueler

Table of Contents

Introduction	4
Materials Used	5
Testing Methods	5
Results	8
Conclusion	10

We personally would like to thank Midwest Prototype for giving us this opportunity. We hope to continue working within the near future.

Introduction

There are countless options when choosing a biomaterial. Some may be more specialized in a certain qualification such as flexibility or thermal resistance while others may promote cellular adhesion. Currently, the team is in need of a material that minimizes protein adsorption as much as possible due to the nature of the project the team is currently working on. For the privacy of the client, the details of what this project fully entails is irrelevant.

At a certain time-point in the Fall 2019 semester, the team required several 3D printed models of a microfluidic device using a non-protein adsorbing material. Fortunately, Midwest Prototype was very willing to provide assistance with this matter. The biomaterials elastomeric polyurethane (EPU-40) and silicone (SIL-30) were capable of completing the task at hand. However, the main issue arose in determining which material was less adsorbent than the other. Midwest Prototype allowed the team to have the 3D printed models at a reduced price in turn for conducting research on the protein adsorption levels of the biomaterials. Using a Biotek Synergy HT plate reader, the team measured the optical density of bovine serum albumin (BSA) with each of the biomaterials over time. Optical density (OD) would enable the team to determine a relative amount of protein adsorption. If OD increases over time, then there is a clear demonstration of protein adsorption. This document contains the methodologies and results found.

Materials Used

- Elastomeric polyurethane
- Silicone 30
- (6%-8%) Bovine serum albumin
- Eppendorf pipette
- 250mL glass beakers
- 96 well plate
- Biotek Synergy HT plate reader

Testing Methods

EPU-40 and SIL-30 were obtained and placed individually into a glass beaker.

Approximately 4 mL of BSA was added to each of the two beakers containing the material and another empty beaker to serve as a control. After a 5 minute interval, an Eppendorf pipette was used to extract three samples from each beaker and placed into the well plate. The Biotek Synergy HT reader measured the maximum optical density of the samples at a wavelength of 280 nm. This process was repeated at a total elapsed time period of 10 minutes, 30 minutes, 1 hour, 2 hours, and 3 hours (Figures 1-6).

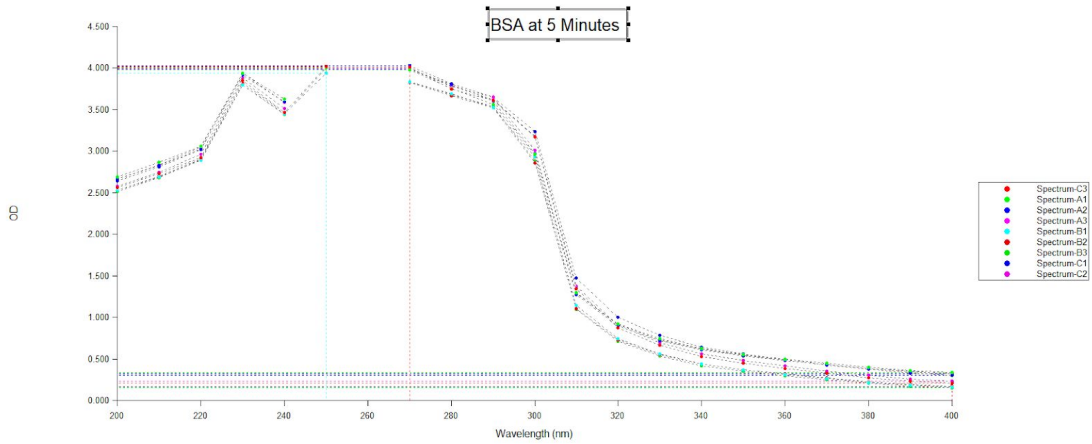


Figure 1: Optical Density of BSA at a total elapsed time of 5 minutes

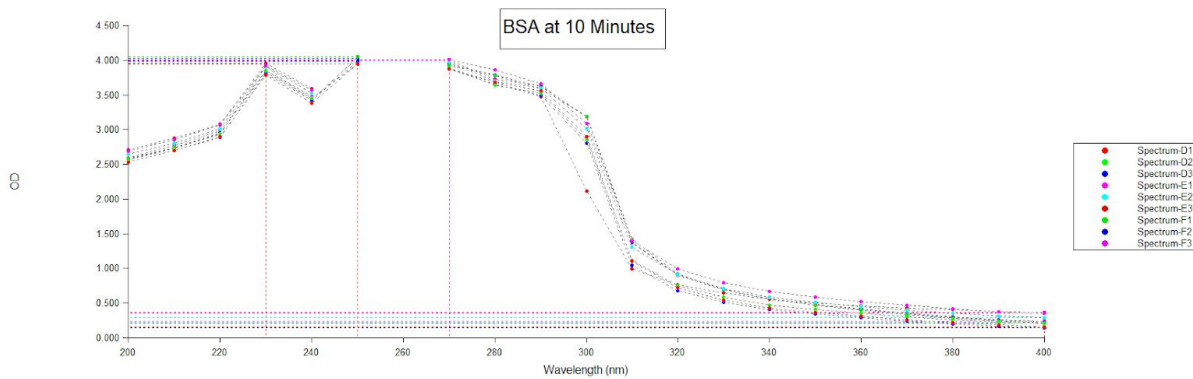


Figure 2: Optical Density of BSA at a total elapsed time of 10 minutes

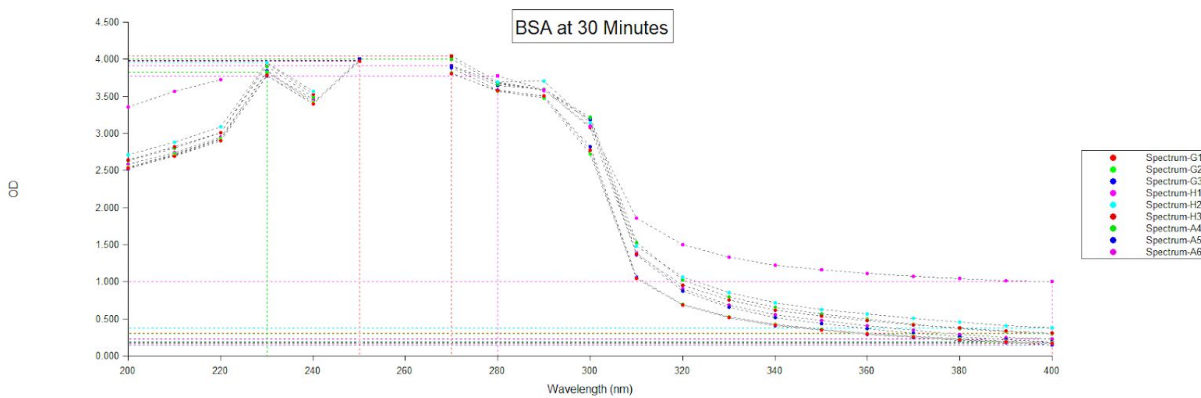


Figure 3: Optical Density of BSA at a total elapsed time of 30 minutes

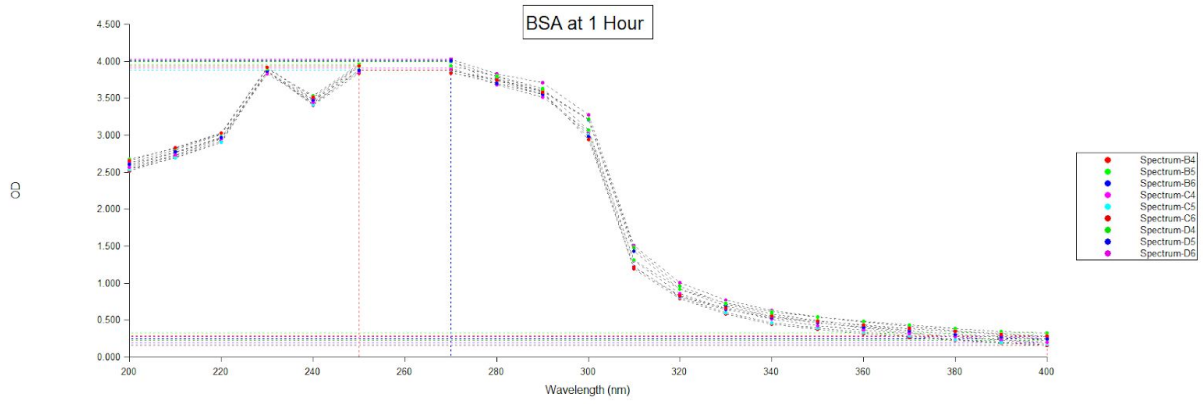


Figure 4: Optical Density of BSA at a total elapsed time of 1 hour

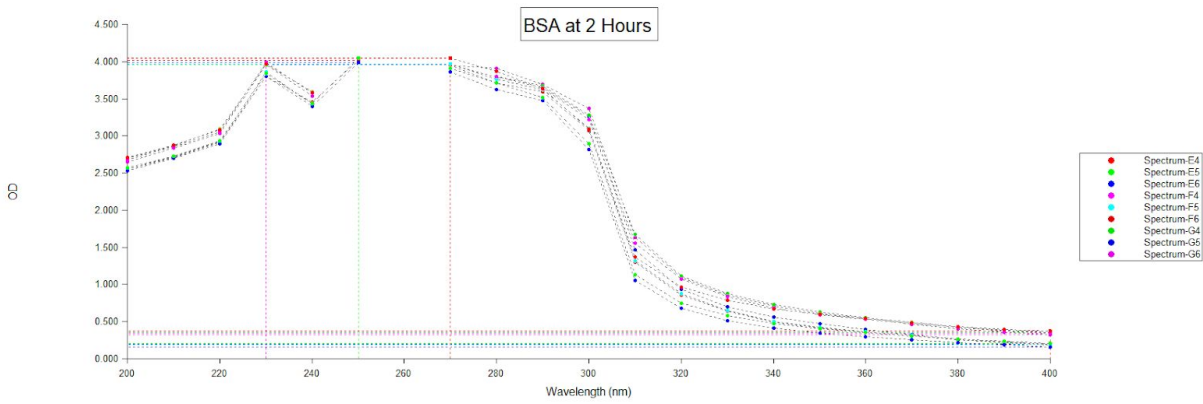


Figure 5: Optical Density of BSA at a total elapsed time of 2 hours

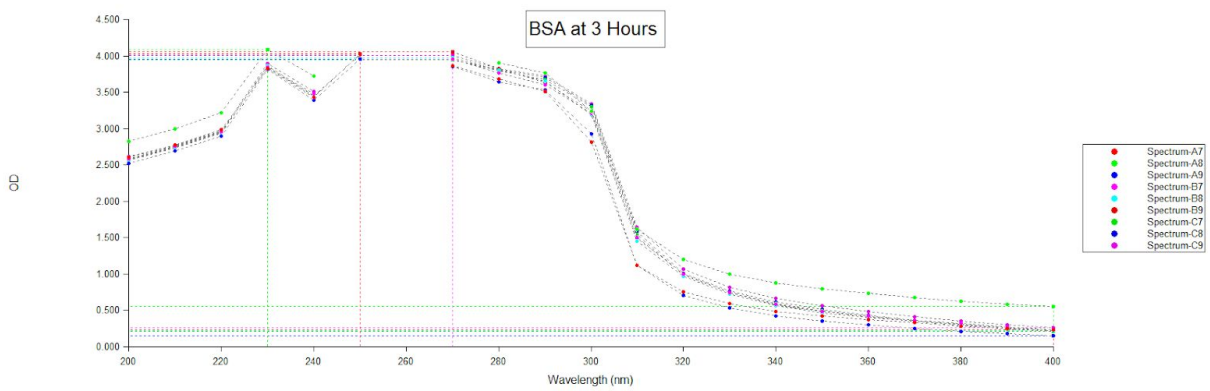


Figure 6: Optical Density of BSA at a total elapsed time of 3 hours

Table 1: All sample OD with their respective material/control and allocated time

Time Elapsed	Material/Control	Sample Maximum Optical Density		
		1	2	3
5 minutes	SIL 30	3.981	3.984	3.992
	EPU 40	3.94	4.021	4.001
	Control	4.028	3.99	4.01
10 minutes	SIL 30	3.95	3.943	3.982
	EPU 40	4.006	3.975	3.961
	Control	4.047	4.029	3.994
30 minutes	SIL 30	3.975	3.824	3.987
	EPU 40	3.773	3.953	4.04
	Control	4.007	4.006	3.917
1 hour	SIL 30	3.934	3.954	4.004
	EPU 40	3.91	3.874	3.878
	Control	3.992	3.874	4.029
2 hours	SIL 30	4.049	4.043	3.987
	EPU 40	3.985	3.968	4.016
	Control	3.959	3.959	3.959
3 hours	SIL 30	4.025	4.084	3.957
	EPU 40	3.954	3.973	4.061
	Control	3.944	4.023	4.006

Results

Upon obtaining the optical density of each sample, an average was taken and graphed over time (Figure 7). As shown, both EPU-40 and SIL-30 share the same characteristic increase in optical density which signifies that there was a level of protein adsorption. A couple of t-tests were conducted on the optical densities of EPU-40, SIL-30, and the control BSA solution.

Between EPU-40 and control, a p-value of 0.1743 was obtained. Between SIL-30 and control, a

p-value of 0.6984 was obtained. Using a significance level of 0.1, both tests fail to reject the null hypothesis, suggesting that there is no significant difference between each biomaterial and control BSA. Likewise, a third t-test was conducted between EPU-40 and SIL-30 in which a p-value of 0.3362 was obtained. Again, using a significance level of 0.1, the null hypothesis fails to be rejected.

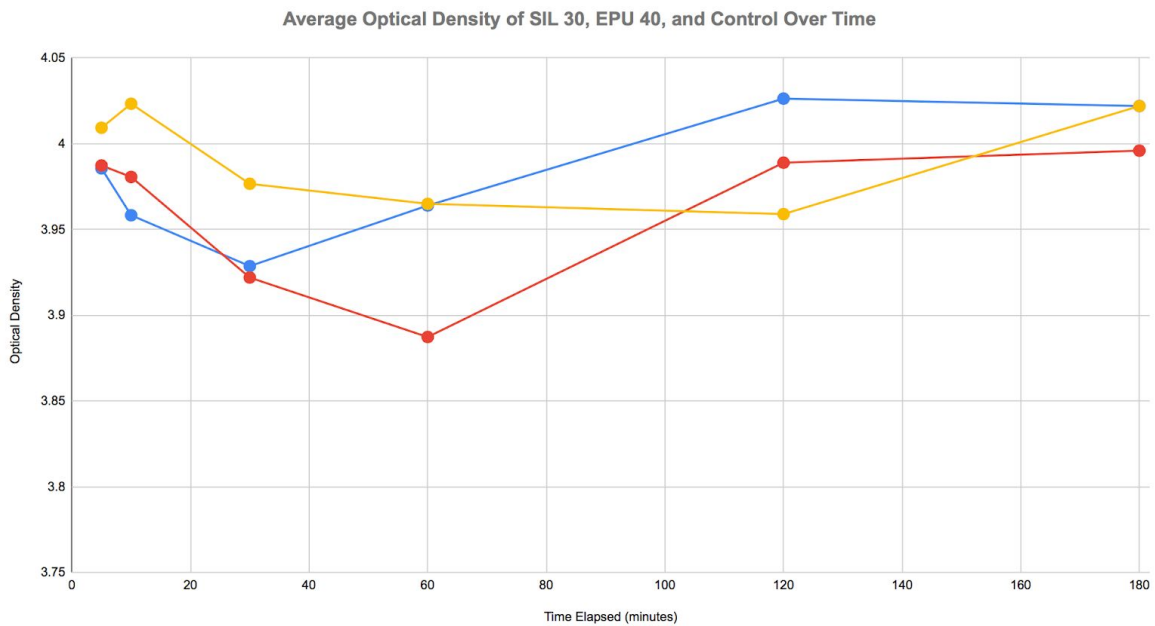


Figure 7: Graph of average optical densities over time. The yellow, blue, and red lines represent control, SIL-30, and EPU-40 respectfully.

Table 2: Statistical data of each biomaterial and control

Time Elapsed (min)	SIL-30 OD Averages	EPU-40 OD Averages	Control OD Averages
5	3.985666667	3.987333333	4.009333333
10	3.958333333	3.980666667	4.023333333
30	3.928666667	3.922	3.976666667

60	3.964	3.887333333	3.965
120	4.026333333	3.988966667	3.959
180	4.022	3.996	4.022
AVG	3.980833333	3.960383333	3.992555556
Standard Deviation	0.05549165279	0.06877435398	0.04452776911
Variance	0.003079323529	0.004729911765	0.001982722222
T-test (control)	0.6984126497	0.1743441487	n/a
T-test (comparing EPU 40 with SIL30)		0.3361640262	n/a

Conclusion

Based on the information obtained, the team found that there was no statistical advantage of one material over the other. However, both biomaterials did show signs of minor protein adsorption. Given the crude nature in which protein adsorption was determined, the team would elect that the methodology used was not the most optimal. A more in depth analysis and conclusion may be reached by utilizing immunofluorescence and measuring the proteins directly on the biomaterial instead.